MECHANICAL EFFECT AND DISSIPATIVE PROCESSES ACCOMPANYING AN EXPLOSION IN A POROUS MEDIUM

E. E. Lovetskii, A. M. Maslennikov, and V. S. Fetisov

UDC 534.222

Experimental and theoretical investigations show that the presence of gas or liquid in rocks has a significant effect on the dynamics of phenomena accompanying failure of a camouflet cavity formed by an underground explosion. In the present work, based on numerical and approximate analytical solutions of the problem, quantitative characteristics of this effect are presented.

1. Failure of a Gas Cavity in a Saturated Porous Medium with Irreversible Volume Deformation. In [1], the influence of water on the mechanical effect of underground explosions is investigated with the help of the water-head model. It is established that an increase in the quantity of water in rocks leads to a noticeable increase in peak pressures at the front of the compression wave. In [2], failure of a cavity in a gas- and water-saturated elastoplastic medium was investigated assuming equal pressures in all components. At the same time, experimental and theoretical investigations [3-6] indicate that such an assumption is well justified at pressures exceeding several kilobars. Starting with the smallest stresses, the picture of volume deformation of the medium, apparently, is as follows. At first, as the stresses applied to the porous medium increase, the solid framework assumes the main load. At this stage, the pressure in it is significantly higher than in the substance saturating the pores, and the bulk compression modulus of the medium as a whole is nearly equal to the bulk compression modulus of the solid component. With a further increase in stress, the solid framework begins to fail and the pores begin to fill up. At the same time, the compressibility of the porous medium can increase sharply (by an order of magnitude). Models of rocks that are based on the assumption of plastic filling of pores [4-6] agree satisfactorily with the experimental data on hydrostatic compression of porous rock [4, 5]. The pores continue to fill up until the increasing pressure inside the pores and the pressure in the matrix are approximately unequal given the applied load. (The pressure cannot equalize completely due to the strength properties of the matrix [4-6]; however, $\Delta p/p \ll 1$, where Δp is the difference in the pressures in the matrix and pore, p is the external pressure applied to the medium.) Further increase in stress is equally absorbed by the interstitial substance and the matrix. This leads to an increase in the bulk compression modulus of the medium. According to [4-6], taking into account the different pressures in the pore and matrix at all stages of loading and unloading leads to irreversible compaction of the medium, observed experimentally [3, 4]. In this case, at the unloading stage, the interstitial matter due to the strength properties of the matrix turns out to be overcompressed compared to the matrix itself. We note that the model of the medium with equal pressures in all components, used in [1, 2], does not describe the irreversible nature of the bulk deformation of porous media.

In this paper, the problem of the expansion of a cavity produced by a camouflet explosion in a gas- and water-saturated elastoplastic medium having the property of irreversible volume compression described above is solved numerically. The irreversibility of the compression is described by taking into account the different pressures in a pore and in the solid matrix both with loading as well as with unloading of the medium. It should be noted that the existing irreversibility of volume deformation is related to the process of hydrostatic compression of the porous medium. Taking into account the possible volume stresses stemming from the plastic shear of the medium (dilatancy effect) is an independent problem and is not investigated in the present work.

The peak pressures as a function of distance from the center of the explosion, the dependence of the maximum radius of the cavity, the plasticity radius as a function of porosity, and the profiles of the shock waves are obtained. It is shown that in a porous medium the shock wave is transformed into a continuous compression wave. The distribution of the residual threshold pressure is obtained for a water-saturated medium.

Assume that initially there is a spherical cavity with radius a_0, in which the energy W of an explosion is liberated suddenly in a space occupied by a saturated porous medium. We will assume that the initial pressure

Moscow. Translated from Zhurnal Prikladnoi Mekhaniki i Tekhnicheskoi Fiziki, No. 2, pp. 126-149, March-April, 1981. Original article submitted February 8, 1980.

0021-8944/81/2202-0248$07.50

in the cavity equals 700 kbar. We will assume that the substance in the cavity is an ideal gas with an adiabatic index $\gamma=1.4$. Generally speaking, the adiabatic index changes as the cavity expands. However, we will neglect the change in the quantity γ, turning our attention first to the qualitative aspects of the behavior of a saturated porous medium with an explosion and to the dynamics of its development. In order to describe a spherically symmetrical motion of the medium, we will use the hydrodynamic equations that take into account the strength effects. The starting equations in Euler variables have the form

$$\frac{\partial v}{\partial t}+u\frac{\partial v}{\partial r}=v\left\{\frac{\partial u}{\partial r}+2\frac{u}{r}\right\},\quad \frac{\partial u}{\partial t}+u\frac{\partial u}{\partial r}=v\left\{\frac{\partial \sigma_r}{\partial r}+2\frac{\tau}{r}\right\},\tag{1.1}$$

$$\frac{\partial e}{\partial t}+u\frac{\partial e}{\partial r}+p\frac{\partial v}{\partial t}+pu\frac{\partial v}{\partial r}=\frac{2}{3}\tau v\left\{\frac{\partial u}{\partial r}-\frac{u}{r}\right\}.$$

The first equation in the system (1.1) is the equation of continuity, the second and third equations are the equations of motion and energy, respectively. Here, v and e are the specific volume and specific energy of the multicomponent medium; u is the velocity; σ_r and σ_φ are the radial and angular components of the stress tensor; $\tau=\sigma_r-\sigma_\varphi$ is the shear stress; $p=-(\sigma_r+2\sigma_\varphi)/3$ is the pressure; t is the time; r is the Euler coordinate.

The systems of equations (1.1) is closed by the elastoplastic relations and the equation of state of the porous medium. We will describe the mechanical properties of the medium in the elastic region by Hooke's law

$$\frac{\partial \tau}{\partial t}+u\frac{\partial \tau}{\partial r}=2G\left\{\frac{\partial u}{\partial r}-\frac{u}{r}\right\},\tag{1.2}$$

where G is the shear modulus of the porous medium. In the plastic zone, we will use Tresca's yield criterion, where

$$|\tau|=\sigma^*=\text{const},\tag{1.3}$$

σ^* is the yield stress. Describing the plastic properties of the medium within the framework of the model of ideal plasticity (1.3), we thereby neglect the dry friction inherent to soil. However, taking into account the plastic properties of the material in the form (1.3) is the simplest procedure and permits describing the basic qualitative laws governing the dynamics of the development of the explosion in a gas–water-saturated medium. Let us make the following comments concerning the stress tensor σ_{ij}, used in (1.1)-(1.3). The quantity σ_{ij} is a complete stress tensor acting on the element of the porous medium. In its turn, σ_{ij} can be related to the stresses $\sigma_{ij}^{(1)}$ acting on the solid component and pressure of the gas or fluid q filling the pores [7]:

$$\sigma_{ij}=(1-m)\sigma_{ij}^{(1)}-mq\delta_{ij},\tag{1.4}$$

where m is the porosity; δ_{ij} is Kronecker's symbol. Performing a convolution of the tensor relation (1.4), we obtain that the total pressure in the medium p is related to the pressure in the matrix $p^{(1)}$ and in the pore q by the relation

$$p=(1-m)p^{(1)}+mq.\tag{1.5}$$

The expansion of the gas cavity with a camouflet explosion assuming that $p^{(1)}=q=p$ was investigated in [2]. However, as shown above, for low pressures the difference between $p^{(1)}$ and q, which leads to irreversibility of the deformation of volume compression, must be taken into account in order to describe correctly the deformation of the medium. In the present work, in order to describe the irreversible nature of the volume deformations of the medium taking into account Eq. (1.5) we used the model of a multicomponent medium proposed in [6], which is a generalization of [4, 5] to the case of compressed matrices and substances filling a porous space. According to [6], this model of the medium describes satisfactorily the behavior of porous gas–water-saturated rocks with loading and unloading. For an equation of state of a porous medium [6], it is necessary to give a number of parameters characterizing the material of the matrix and the liquid or gas that saturates the pores. We choose the following microscopic parameters of the matrix: density 2.65 g/cm^3; plastic velocity of sound $c_0=4500$ m/sec; shear modulus $G_m=100$ kbar, shear strength $Y=1$ kbar. As the interstitial liquid, we chose water with the parameters for the equation of state taken from [8]. According to [4-6], the parameters G_m and Y describe the deformation of a medium in the vicinity of a pore, whose dimensions we will assume are much less than the average size of the pieces into which the medium is fractured with macroscopic plastic shear and are the characteristic microparticles or grains of which the medium consists. According to [9], for most possible scales of explosions this estimate is justified. The shear deformation of the medium in the immediate vicinity of a pore in the general case may not be related to the shearing deformation of the medium as a whole (e.g., with hydrostatic pressure), so that the microscopic plastic flow should be described by constants that differ from G_m and Y. According to the work described in [10], wherein an experimental study was conducted of the dependence of the parameters of dynamic compression of NaCl as

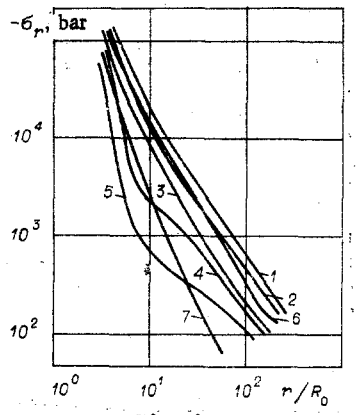

Fig. 1

a function of porosity, the macroscopic strength of the medium decreases with an increase in porosity. For this reason, the quantity σ^*, entering into (1.3), was chosen in the calculations to be less than Y. We note that with the assumptions made concerning the sizes of the pieces of fractured rock, the elastoplastic behavior of the medium as a whole will not have a significant effect on the change in porosity (the pore sample with macroscopic shear will be taken along the boundaries of the fractured pieces, whose dimensions are taken as significantly greater than the average pore sizes). For this reason, it may be assumed that the equation of state of the medium does not depend on the shearing deformations of the medium as a whole.

For a numerical calculation, the system of equations (1.1)-(1.3), rewritten in Lagrangian coordinates, was replaced by a system of finite difference equations. The difference scheme, similar to the scheme in [11], had second-order accuracy with a uniform Lagrangian grid. In order to smooth the hydrodynamic discontinuities, a linearly quadratic artificial viscosity was introduced into the difference equations, which permitted direct computation. The stability of the calculation was ensured by an appropriate choice of the time step chosen. The initial conditions were given as the pressure in the initial cavity and the values of v, p, and e in the surrounding soil. The velocity u at $t=0$ was everywhere assumed to equal zero. The boundary conditions were given at the center (for $i=0$) and in front of the shock-wave front. Part of the spatial grid was located in the gas cavity, which permitted taking into account the complex gasdynamic picture of the motion of the gas in the cavity.

Numerical calculations were carried out for $G=100$ kbar, $\sigma^*=150$ bar, and $p_\infty=200$ bar (p_∞ is the background pressure in the medium). Figure 1 shows the maximum radial stress $|\sigma_r|$ on the shock-wave front as a function of distance to the gas cavity for media with different porosity and different substances saturating the pores (gas or water). Curve 1 corresponds to the case of a nonporous medium, 2 and 3 correspond to the case of a porous water-saturated medium with a porosity m equal to 7 and 23%, respectively. Curves 6 and 7 are taken from [2] and presented here for comparison with the results of the present work. Curve 6 corresponds to a water-saturated medium with $m=23\%$ and curve 7 corresponds to a gas-saturated medium with $m=7\%$. Both curves were obtained from numerical calculations assuming equal pressures in all components of the medium. From an analysis of curves 1-5, it is evident that as the porosity increases, the amplitude of the shock wave decreases significantly. This is especially noticeable in a gas-saturated medium. The curves corresponding to a medium with gas have a characteristic deviation that leads to less damping of the wave at small amplitudes. This deviation is related to the change in the propagation regime of the wave. The region of the curves above the deviation corresponds to the case when the pores are filled up along the shock-wave front. This regime, according to [8], is characterized by significant dissipative processes and, in particular, by high shock-induced heating of the medium. At lower pressures, according to the model chosen for the medium [4-6], the main load is absorbed by the solid framework and the pores are not filled up. In this case, energy dissipation decreases sharply, which leads to less damping of the wave itself. The curves for the water-saturated medium behave similarly; however, due to the fact that there is relatively little flow into pores filled with water, no sharp deviation is observed. If the results of this work are compared with curves 6 and 7, then one can see that for the water-saturated medium there is good agreement between the calculations (curves 3 and 6) in the stress range $|\sigma_r| > 1$ kbar. For the gas-saturated medium with $|\sigma_r| > 1.5$ kbar, there is also good agreement with calculations according to both models. With lower stresses, curve 7 decreases with the same slope, since according to the equal-pressure model the regime in which the pores collapse will occur at practically all stresses due to the small bulk compression modulus of the gas in the pores. Curve 5 at small stresses is significantly higher than curve 7. The amplitude of the elastic wave in this case is 5-10

times greater than the amplitude calculated according to the equal-pressure model. This indicates that for a gas-saturated medium with microparticles and grains having a high strength, the equal-pressure model cannot be used for describing the damping of a small-amplitude wave.

It should be noted that on curves 4 and 5 in Fig. 1, immediately after the deviation there is a region in which the damping of the wave is weaker than even the damping in the elastic zone for lower stresses. This effect is related to the restructuring of the wave profile as it passes from the medium with high compressibility into the low-compressibility medium. The physics of this process is similar to that described in detail in [12]. (In the present work, we consider rocks that have low compressibility for low stresses and for high stresses their compressibility can increase considerably due to pore filling, which is what leads to the pressure dependence of the physical boundary in the behavior of the substance and the properties of the wave in proportion to the damping of the wave amplitude.)

Taking into account different pressures in the matrix pores leads to a degeneration of the shock wave into a continuous compression wave. This is clearly seen in Fig. 2a, b, where the profiles of the stress waves are shown for the water-saturated and gas-saturated media, respectively. Fig. 2a, curve 1 corresponds to a nonporous medium and to the time $\lambda = t/t_0 = 3$ ($t_0 = a_0/c_0$, c_0 is the plastic velocity of sound in the solid framework). Curves 2 and 3 correspond to the water-saturated porous medium with m = 7% and are defined at times $\lambda = 3$ and 7, and in addition, curve 2 is computed according to the equal-pressure model. All curves in Fig. 2a correspond to the distance $r/a_0 = 32$ from the center. It is evident that as the porosity increases the amplitude of the wave and its velocity of propagation decrease considerably. Taking into account different pressures in the matrix and in the pore (curve 3) leads to considerable washing out of the leading front of the wave. This effect is manifested even more strongly for the gas-saturated medium (Fig. 2b). All curves in Fig. 2b are constructed for a medium with m = 7%. Curve 1 corresponds to $\lambda = 1$; curve 2 to $\lambda = 2.7$; curve 3 to $\lambda = 5.4$; and curve 4 to $\lambda = 2.7$. Curve 4 is a calculation according to the equal-pressure model and is presented for comparison. Curve 1 clearly shows the shock-wave front, but the stress wave, corresponding to compression of the medium with low pressures, is already separating out at this time from the base of the wave in the forward direction. This is related to the fact that at low pressures the main stress is absorbed by the framework, and for this reason, the medium has a higher modulus of volume compression than at higher stresses, when the pores begin to fill up and the compression modulus drops sharply [4-6]. The shock wave corresponding to irreversible pore filling damps out with time and the compression wave moves away into the forward direction. Thus, there is a transition from the shock-wave regime (curve 1) to a continuous compression wave (curve 3). It should be noted that in the equal-pressure model (curve 4), the wave profile is not transformed, it always damps out in the shock-wave regime. This is what leads to lower elastic wave amplitudes in this model, which was discussed above.

In this work, we study the effect of porosity on the dimensions of the failure zone and the size of the cavity as a function of the explosion. Figure 3 illustrates the plasticity radius R_1, which within the framework of the chosen model for the elastoplastic behavior of the medium (1.2) and (1.3) is associated with the radius of the failure zone, as a function of the porosity m. Curve 1 corresponds to a water-saturated and curve 2 to a gas-saturated medium. As the porosity increases, the plasticity radius R_1 decreases, and in addition, this decrease is more noticeable for the gas-saturated medium. Fig. 4 shows the maximum radius of the cavity a_{max}/a_0 as a function of the porosity m (curve 1 corresponds to a porous medium with water and curve 2 with gas). Just as R_1, a_{max} decreases with increasing m, and in addition, this decrease is greater for a medium

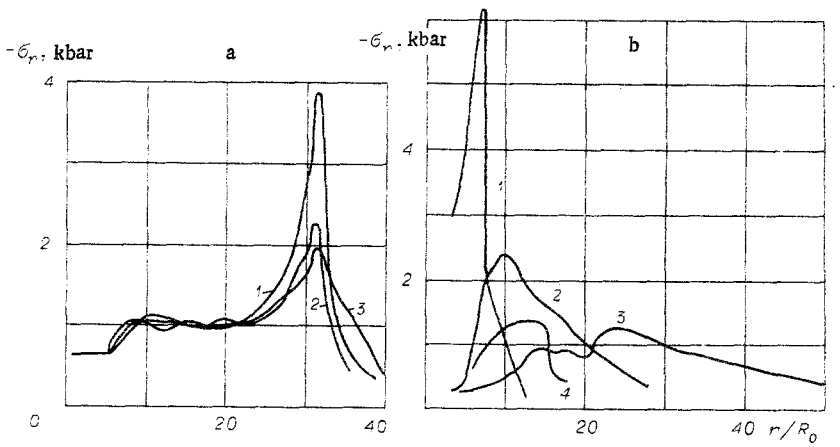

Fig. 2

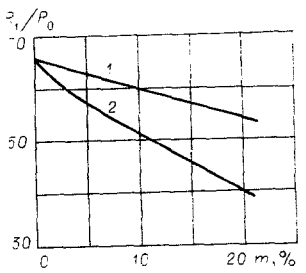

Fig. 3

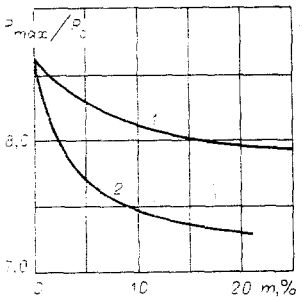

Fig. 4

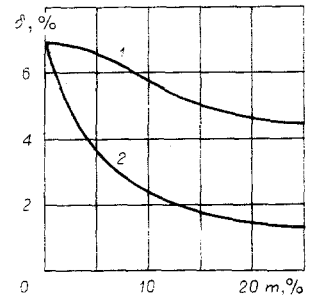

Fig. 5

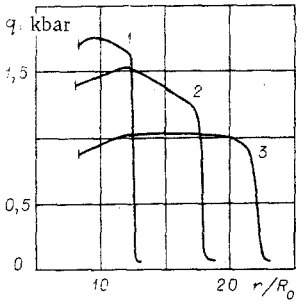

Fig. 6

with gas. A characteristic property of both curves in Fig. 4 is the steeper drop in a_{max} for low porosities ($m \leq 10\%$). For large values of m the curves decrease, but more smoothly at this point, as if they have become asymptotic. This dependence of the quantity a_{max} on m can be understood if the change in the dissipative processes as a result of an explosion with an increase in porosity m is analyzed. As calculations show, in a nonporous medium, the basic mechanism for dissipating the energy of the explosion (up to 50%) is plastic flow. A large fraction of the energy in the explosion (up to 40%) at the initial stage of the cavity expansion is transferred in the form of kinetic energy to the medium surrounding the cavity. Computational results indicate the fact that due to gas pressure the cavity expands only at the earliest times ($\lambda < 3$). Further expansion occurs mainly due to inertia, due to the kinetic energy stores in the medium surrounding the cavity. This motion becomes slower as energy is dissipated until the cavity stops increasing. At the same time, the cavity overshoots the equilibrium position corresponding to quasistatic expansion. In a porous medium, as the calculations performed and experimental data [13] show, dissipation of the energy in the explosion into heat is greater than in a nonporous medium and is related mainly to shock heating of matter. In this case, the fraction of the kinetic energy in the porous medium decreases. This decrease in the kinetic fraction of the total energy of the explosion $\delta = E_{kin}/W$ at the time the cavity stops expanding is shown in Fig. 5, where curve 1 corresponds to a water-saturated and curve 2 to a gas-saturated medium. The greatest decrease in the quantity δ is observed in the porosity range $0 < m < 15\%$, when there is a change in the basic dissipative mechanisms (plastic to shock). The decrease in the quantity δ and, therefore, the inertial forces leads to a decrease in the values R_1 and a_{max}, as noted above.

The model of the equation of state of the medium with irreversible volume deformation used in this work [6] yields the pore pressure distribution at times when expansion of the gas cavity has already been completed. Figure 6 shows the pore pressure q as a function of the distance for a water-saturated medium. Curve 1 corresponds to $m = 2.7\%$; curve 2 to 7% and curve 3 to 22%. As can be seen from this figure, as a result of the explosion, a zone with high pore pressure is formed. According to [4-6], its origin is related to the partial pore filling at the compression phase as the shock wave passes. To the left of the region with high pore pressure, there is a gas cavity formed during the explosion and to the right a medium in which the pores are not filled, which is what leads to the sharp drop in pressure on the right boundary of the region. As the porosity increases, the size of the zones with high pore pressure increases and the magnitude of the residual pore pressure decreases simultaneously. The presence of the zone described above can have an important effect on filtration processes after the explosion.

2. Dissipation of the Energy of an Explosion in a Porous Medium with Irreversible Volume Deformation. A considerable part of the energy of an explosion in a solid medium is dissipated in the matter surrounding the

explosive charge. The energy in the explosion is dissipated on the shock-wave front during plastic flow of matter behind the front. Part of the energy is transformed into energy of residual elastic deformations. A small fraction of the overall energy in the explosion is emitted in the form of elastic waves. Many real rocks are porous with some degree of gas–water saturation. For this reason, the problem of energy losses with an explosion in porous saturated media is of considerable interest [8].

The problem of energy dissipation with an explosion in a porous medium that is deformed plastically was studied theoretically in [14, 15]. The analysis carried out in these works is limited to the case of complete collapse of empty pores on the shock front. The substance behind the shock-wave front was assumed to be incompressible. For a more complete and exact description of the explosion, it is necessary to take into account the variable compressibility of the medium on the shock front and stress relief behind the front. Here, irreversible volume deformations are a characteristic property of porous media [3, 16]. At this point, we examine the distribution of the energy of a camouflet explosion in a saturated porous medium taking into account this irreversibility.

We will study the energy characteristics of the explosion, the effect of the strength parameters of the medium, porosity, and the nature of pore saturation on these characteristics. This analysis is carried out with the help of a numerical solution of the system of hydrodynamic equations (1.1)-(1.3) taking into account the shear strength of the medium. However, at this point, in contrast to the first case, instead of condition (1.3) we use the condition for Coulomb's plasticity

$$|\tau| = \sigma^* + kp, \tag{2.1}$$

where σ^* characterizes the coupling; k is the increase in strength of the medium with hydrostatic compression. According to [3, 16], relation (2.1) describes satisfactorily the behavior of rocks under shear stresses. The multicomponent nature of the medium is taken into account with the help of a model equation of state described in Sec. 1.

The energy characteristics of the medium with the camouflet explosion variants that were checked are presented in Table 1. Here

$$E_1 = 4\pi \int \rho \frac{u^2}{2} r^2 dr$$

is the kinetic energy of the medium (the integrals in E_1, E_2, E_4, and E_5 are taken over the disturbed region); $E_2 = 4\pi \int dt \int \frac{2}{3}\tau\left(\frac{\partial u}{\partial r} - \frac{u}{r}\right) r^2 dr$ is the energy dissipated due to plastic flow; τ is the shear stress due to plastic flow of the medium; $E_3 = 2\pi \int p_H \varepsilon_H r^2 dr$ is the energy dissipated into heat on the shock front; p_H and $\varepsilon_H = 1 - \rho_0/\rho_H$ are the pressure and compaction of the medium on the shock fronts; ρ_H is the density of the medium on the shock front; $E_4 = E_2 + E_3$ is the total thermal energy in the medium; $E_5 = \frac{4}{3}\pi \int \frac{\tau^2}{2G} r^2 dr$ is the energy of elastic shear deformations in the medium; $E_6 = 4\pi \int \frac{p^2 - p_\infty^2}{2K} r^2 dr$ is the energy of volume compression of the medium; K is the bulk compression modulus of a multicomponent medium; p_∞ is the backward pressure; $E_7 = E_5 + E_6$ is the total elastic energy stored in the medium; E_8 is the energy of the gases inside the cavity.

In Table 1, the upper numbers in each line indicate the fraction of the corresponding energy with respect to the total energy of the explosion (all values are given in percent). The lower numbers indicate the fraction of the corresponding energy with respect to the energy transmitted to the medium surrounding the cavity, i.e., to the total energy of the explosion minus the energy of the detonation gases inside the cavity. In what follows, we will make comparisons with the lower numbers unless otherwise specified. The data in Table 1 are presented for a time when the cavity has attained its maximum radius. However, since the return motion of the cavity for the chosen strength parameters (see Table 1) is not large ($< 5\%$ for all variants), the numbers characterizing the distribution of energies E_1, E_2, E_3, E_4, and E_8 vary little with the return motion of the cavity. The value of E_5 depends considerably on the return motion, which is discussed in greater detail in what follows.

In carrying out the calculations according to the technique indicated above, we varied the coupling parameters σ^* and the strengthening coefficient k, the magnitude of the back pressure p_∞, the initial porosity of the medium, and the nature of the saturation of the porous space (gas or liquid). The variants of the computations 1-6 correspond to the case of a monolithic medium with 0 porosity. They show that for a monolithic medium most of the energy of the explosion was dissipated with the plastic flow. An increase in σ^* leads to a weak increase in energy E_2 and decrease in E_3. On the whole, however, the quantity $E_4 = E_2 = E_3$ varies little. As

TABLE 1

Variant No.	Type of medium	m, %	σ^*, bar	k	p_∞, bar	E_1	E_2	E_3	E_4	E_5	E_6	E_7	E_8
1	Monolith	—	150	—	180	6,3 6,9	36 40	28 31	64 71	6,0 6,6	14 15,4	20 22	9,3
2	»	—	150	—	300	6,0 6,7	32 36	29 32	61 68	5,3 5,9	18 20	23,3 26	10
3	»	—	300	—	300	6,8 7,8	35 40	25 29	60 69	6,7 7,7	14 16	20,7 23,7	12,5
4	»	—	150	0,1	200	4,6 5,2	47 53	21 24	68 77	4,4 5,0	11 12,5	15,4 17,5	11,5
5	»	—	150	0,3	200	4,0 4,7	50 58	22 25	72 83	3,3 3,8	7,3 8,5	10,6 12,3	14
6	»	—	150	0,6	200	4,0 4,7	50 59	21 25	71 84	2,7 3,2	6,3 7,5	9,0 10,7	16
7	Porous with liquid	12	150	—	100	4,7 5,2	32 35	42 47	74 82	5,5 6,1	6,2 6,9	11,7 13	10
8	»	12	300	—	—	5,1 5,8	35 40	38 43	73 83	6,6 7,5	2,6 3,0	9,2 10,5	12,5
9	»	12	300	—	100	5,1 5,9	33 38	38 44	71 82	6,2 7,1	4,4 5,1	10,6 12,2	13
10	»	12	300	—	320	5,0 5,8	28 32	40 46	68 78	5,6 6,4	7,5 8,7	13,1 15,1	13,5
11	»	23	150	—	185	4,0 4,5	28 32	46 52	74 84	4,5 5,1	5,8 6,5	10,3 11,6	11,5
12	Porous with liquid*	23	150	—	185	3,2 3,6	27 31	49 55	76 86	4,5 5,1	4,5 5,1	9,0 10,2	11,5
13	Porous with gas	2,7	150	—	220	4,2 4,8	25 28	44 50	69 78	4,3 4,8	11,0 12,5	15,3 17,3	11
14	»	2,7	300	—	250	4,3 5,0	26 30	43 50	69 80	4,9 5,7	8,0 9,3	13 15	13,5
15	»	12	150	—	180	1,9 2,2	17 20	62 71	82 94	2,6 3,0	3,6 4,1	6,2 7,1	12,5

*Y = 500 bar.

the parameter σ^* increases, the fraction of the kinetic energy E_1, which can be associated with the kinetic energy of the elastic wave, increases as well. The increase in E_1 stems from the fact that as σ^* increases the amplitude of the elastic wave increases. The elastic energy of volume deformation E_6 decreases with an increase in σ^*. As calculations show, this is related to the fact that as σ^* increases the stress wave becomes considerably narrower (higher harmonics predominate in its frequency spectrum) with a weakly increasing wave amplitude. This leads to a decrease in the region where the medium undergoes strong volume compression and, therefore, to a decrease in the magnitude of the energy E_6. In contrast to E_6, the quantity E_5 increases with an increase in σ^*, so that the magnitude of the shear stresses increases.

In calculating explosions in a monolithic medium, we varied the strengthening parameter of the medium k. The results of the calculations show that small values of k have the sharpest effect on the dissipative processes (compare variants 1 and 4 in Table 1). Comparison of variant 4 and 5 and 6 shows that further increase in k has a less noticeable effect on the dissipative processes. The results of the calculations show that the magnitude of the cavity expansion is determined by two mechanisms. The first one, call it a quasistatic mechanism, is related to the expansion of the cavity due to the pressure of gases present in the cavity. This expansion continues until the strengthening forces of the medium surrounding the cavity no longer balance the gas pressure in it. The second mechanism, which we will refer to as dynamic, stems from the available kinetic energy stored in the medium surrounding the cavity. Moving out from the center, the medium permits the cavity to expand. The higher the initial kinetic energy stored in the medium, the greater will be the size of the cavity with other parameters of the problem remaining unchanged. The time dependence of the energy E_1 is given in [17]. It is shown that the maximum value of E_1 occurs at the earliest times during the expansion

of the cavity due to the energy of the gases in the cavity. Later on, the dissipative processes in the medium decrease the magnitude of E_1, and the efficiency of the dynamic mechanism for the expansion of the cavity is determined according to how this dissipation proceeds. As a whole, taking into account the quantity k leads to a decrease in the values of the energy E_1 at initial cavity expansion times as well as at later times (the high strength during the initial cavity expansion, when high pressure leads to a lower acceleration of the medium surrounding the cavity) and to a greater plastic energy dissipation. This leads to a decrease in the efficiency of the dynamic mechanism for cavity expansion (therefore, to a smaller cavity radius) and to a decrease in E_5 and E_6. The results of the calculations for the medium with zero porosity indicate the fact that the dominant mechanism for energy dissipation in the cavity is plastic flow. We note that this result coincides with the conclusions in [14, 15, 17].

The variants 7-12 of the computations correspond to the case of a porous medium saturated with liquid. All the conclusions arrived at above for the dependence of the dissipation of the energy in the explosion on the parameter σ^* are valid as well for saturated porous media with the single difference that these dependences are less strongly manifested. Calculations for porous rock saturated with liquid show that a considerable fraction of the energy in the explosion is dissipated on the shock front (~40-55%). The energy E_3 exceeds by 10-15% the energy E_2, which determines the dissipation in the medium with zero porosity. The effect of the back pressure p_∞ on the dissipative processes during the explosion can be understood from the calculations 8-10. From these it can be seen that the back pressure has the greatest effect on the quantity E_6, which is understandable considering that the energy E_6 is mainly related to the wave front and is proportional to the difference $p^2-p_\infty^2 = (p+p_\infty)(p-p_\infty)$, while the excess pressure p over the back pressure p_∞ in the wave, as the calculations performed show, is practically independent of the quantity p_∞. For fixed porosity and type of pore saturation, the dependence of the energy E_6 on the quantity p_∞ is linear. For the calculations 8-10, it can be represented in the form

$$E_6 = 3.0 + 18.3p_\infty,$$

where E_6 is expressed in percent and p_∞ in kilobars. It should be noted that the calculation results show also that the magnitude of the energy E_6 is related mainly to the elastic wave front. If we take into account that the total energy of the elastic wave is made up of the kinetic energy and the energy of volume compression in the wave (the contribution of shearing energy is small due to the shear deformations in the elastic wave), then we can conclude that as the magnitude of the back pressure increases, the energy in the elastic waves emitted by the explosion increases (for the variants 8 and 10, the sum E_1+E_6 increases by a factor of 1.5).

Variants 11 and 12 clarify the effect of the parameter Y on the dissipation of the energy of the explosion. Calculation 12 corresponds to a medium with the smallest strength of microparticles that form it with other conditions remaining unchanged. It is evident from the results in Table 1 that variation of Y has little effect on the dissipative processes. Only the values of E_1 and E_5 decrease noticeably with a decrease in Y. Apparently, this is related to the somewhat greater energy dissipation on the shock front. In a porous medium saturated with liquid the thermal energy dissipation as a whole is greater than in a nonporous medium. For a gas-saturated medium, the value of the energy E_4 becomes even greater and can attain 95% of the energy that is given up by the cavity to the surrounding medium.

Variants 13-15 represent calculations in a gas-saturated medium. It is evident from these that a gas-saturated medium is characterized by a lower kinetic energy and lower, even in comparison with a medium saturated with liquid, plastic dissipation. The basic mechanism for dissipation for this medium is dissipation of energy on the shock front due to irreversible pore collapse. The dependences on the parameters σ^* and p_∞ have the same characteristic features as for a nonporous or liquid-saturated medium.

One of the results of the work is the construction of the dependence of each of the dissipative energies entering into Table 1 on the porosity of the medium. These dependences are shown in Figs. 5, 7, and 8. All curves are constructed for values of $\sigma^* = 150$ bar, $k = 0$, $p_\infty = 180$ bar, and characterize dissipative processes with respect to the emitted energy (the lower numbers in each line in Table 1). Curves 1 and 2 in Fig. 5 illustrate the dependence of E_1 on the porosity m for a liquid-saturated and gas-saturated porous medium, respectively. The greatest decrease in E_1 for curve 1 occurs in the porosity range 5-15 vol. %. Low porosities have almost no effect on the radiated kinetic energy. For a gas-saturated medium, the drop in energy E_1 occurs over the entire porosity range, and in addition, the most rapid drop occurs for small values of the porosity. Both curves 1 and 2 for $m > 15\%$ decrease comparatively weakly. This indicates the fact that E_1 becomes practically unchanged for high porosities for a liquid-saturated as well as for a gas-saturated medium. Fig. 7 illustrates the dependence of the energies E_2, E_3, and E_4 on the porosity m (curves 1 and 2 correspond to E_2;

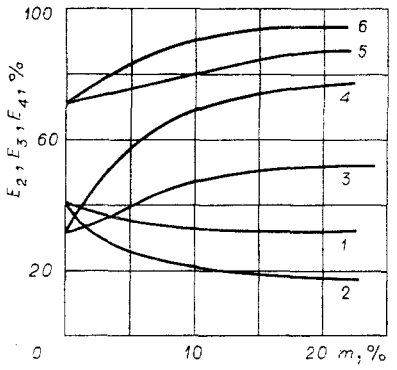

Fig. 7

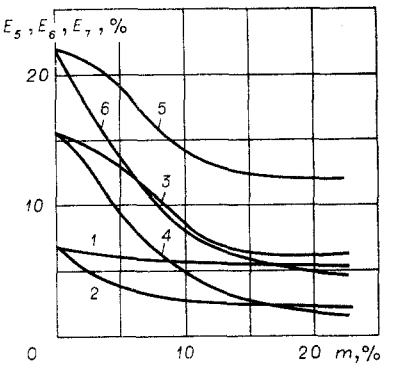

Fig. 8

3 and 4 to E_3; 5 and 6 to E_4, respectively, for the liquid- and gas-saturated medium). The calculations show that the decrease in the value of E_2 and increase in the values of the energies E_3 and E_4 are most sharply manifested in a gas-saturated medium. A characteristic feature of all curves in Fig. 7 is that they are asymptotically independent of porosity. These asymptotes are equal and have the values for curve 1, 31-30%; 2, 15-16%; 3, 52-53%; 4, 79-80%; 5, 86-87%; and 6, 94-95%. This indicates that for high porosity dissipative processes proceed in the same manner and depend mainly on the nature of the pore saturation (gas or liquid). The increase in the magnitude of E_3 is related to the irreversible partial or complete pore collapse on the shock front. The large dissipation of energy on the shock front decreases the efficiency of the dynamic mechanism for cavity expansion, which in turn leads to a lower maximum cavity radius and smaller shear deformations and, therefore, to a lower value of the energy E_2. Fig. 8 shows the elastic energies E_5, E_6, and E_7 as a function of the porosity (curves 1 and 2 correspond to E_5; 3 and 4 to E_6; 5 and 6 to E_7, for liquid- and gas-saturated media, respectively). As can be seen from Fig. 8, the value of the shearing energy E_5 for the liquid-saturated medium is practically independent of the porosity, while for the gas-saturated medium a substantial drop is observed only for low porosities. The volume elastic energy E_6 and the total elastic energy E_7 decrease strongly with an increase in porosity. As calculations show, most of the energy E_5 is concentrated in the immediate vicinity of the cavity. For this reason, it can be a source of secondary elastic waves. The energy E_5 is practically transformed into the cavity energy E_8 with the reverse motion of the cavity.

Analysis of energy dissipation in a saturated porous medium leads to the following results. In contrast to a medium with zero porosity, where the main mechanism for dissipating the energy of the explosion is plastic flow, in a porous medium energy is dissipated primarily on the shock front. The conclusion that there is a considerable increase in the magnitude of the energy E_3 with an increase in porosity is supported by the results of experimental investigations [13]. A large part of the energy of the explosion turns out to be stored in elastic compression and shear deformation energy, and, in addition, the latter is reversible and apparently can become a source of secondary elastic waves after the explosion. As the back pressure increases, the elastic energy of volume compression which is concentrated on the elastic wave front increases, leading to an increase in the energy in this wave. In comparison to the gas-saturated medium, pore saturation by a liquid approximates the energy characteristics of an explosion by an explosion in a medium with zero porosity, i.e., by an increase in the mechanical effect of the explosion. The results of the present work agree qualitatively with the basic conclusions of [17]. There is a noticeable difference only in the decrease in the magnitude of the energy E_1 with increasing porosity. In [17], this decrease is underestimated due to the use of a physical model for the medium with equal pressures in all components, which at low pressures does not describe the fact that the solid framework of the porous medium carries the main load.

3. Dissipation of Energy in the Near Zone with an Explosion in a Porous Medium. Since the amplitude of the shock wave in the direct vicinity of the center of the explosion is large ($\gtrsim 100$ kbar), energy dissipation in the near zone is important. It leads to the formation of zones in which the medium is vaporized and melted and has a large effect on the nature of subsequent wave propagation and damping.

In solving such a problem, it is important to note that with such stresses on the shock front the strength properties of the medium can be neglected and then the only mechanism for thermal losses of energy of the explosion will be shock heating of the medium.

The starting system of hydrodynamic equations describing the explosion assuming spherical symmetry has the following form in Eulerian coordinates:

$$\frac{\partial v}{\partial t} + u\frac{\partial v}{\partial r} = v\left\{\frac{\partial u}{\partial r} + 2\frac{u}{r}\right\}; \tag{3.1}$$

$$\frac{\partial u}{\partial t} + u\frac{\partial u}{\partial r} = -v\frac{\partial p}{\partial r}; \tag{3.2}$$

$$\frac{\partial e}{\partial t} + u\frac{\partial e}{\partial r} + p\left(\frac{\partial v}{\partial t} + u\frac{\partial v}{\partial r}\right) = 0, \tag{3.3}$$

where v and e are the specific volume and specific internal energy of the medium; u is the velocity; p is the pressure; r is the Eulerian coordinate. The system of equations (3.1)-(3.3) is closed by a Mie–Gruneisen equation of state.

In the calculations, the source of the explosion was modeled as a gas cavity expanding according to an adiabatic law with initial size a_0 and initial pressure p_0. Here, a_0 was taken as the radius of formation of the shock wave (the time for formation of the shock wave can be taken [18] as its separation from the front of the thermal wave). The pressure p_0 constituted 8 mbar. The matter in the cavity was assumed to be an ideal gas with constant adiabatic index $\gamma = 1.4$.

The system of equations (3.1)-(3.3) can be solved exactly only by numerical methods. However, in order to attain a qualitative understanding of the effects accompanying the explosion, the system indicated can be solved within the framework of the model in [14] without taking into account the strength properties of the medium. Following [14], let us assume that matter is compressed irreversibly from a density ρ_0 to a density ρ_1 on the shock wave front. This compression is characterized by the parameter $\varepsilon = 1 - \rho_0/\rho_1$. The medium behind the shock wave is assumed to be incompressible. For this reason, the equation of state of the medium and Eq. (3.3) are not directly required for describing the dynamics of the explosion within the framework of this model. The boundary conditions on the cavity $a(t)$ and on the shock front $R(t)$ are as follows:

$$\begin{gathered} u(R) = \varepsilon\dot{R},\ u(a) = \dot{a}, \\ p(R) = (1/\varepsilon)\rho_0 u^2(R),\ p(a) = p_0(a_0/a)^{3\gamma}. \end{gathered} \tag{3.4}$$

In Eqs. (3.4), the back pressure has been omitted, since in examining the initial stage of the explosion it can be neglected. Taking into account the incompressibility behind the shock front it follows from Eq. (3.1) that

$$u = \dot{a}a^2/r^2.$$

Substituting this relation into (3.2), integrating with respect to r and using the boundary conditions (3.4) on the cavity, we obtain the pressure distribution behind the shock front

$$p(r, t) = \rho_1\left(\frac{\ddot{a}a^2 + 2a\dot{a}^2}{r} - \frac{\dot{a}^2a^4}{2r^4}\right) + p_0\left(\frac{a_0}{a}\right)^{3\gamma} - \rho_1\left(\ddot{a}a + \frac{3}{2}\dot{a}^2\right). \tag{3.5}$$

Knowing the laws describing propagation of the shock wave $R(t)$ and the expansion of the cavity $a(t)$, it is possible to calculate with the help of (3.5) the pressure in the zone $a \le r < R$. The function $a(t)$ is obtained by solving the camouflet equation, which is obtained by substituting the boundary condition on the shock front (3.2) into (3.5). The camouflet equation has the form

$$\begin{gathered} \frac{dy}{dx} = \frac{1}{x\left(1 - \frac{a}{R}\right)}\left\{\frac{2p_0}{\rho_1 a_0^2 x^{3\gamma}} - 2y\left[\frac{3}{2} - 2\frac{a}{R} + \frac{2-\varepsilon}{2\varepsilon}\left(\frac{a}{R}\right)^4\right]\right\}, \\ \frac{dt}{dx} = 1/\sqrt{y},\quad x = a/a_0,\quad y = \dot{x}^2,\quad \frac{a}{R} = \frac{\varepsilon^{1/3}x}{[x^3 - (1-\varepsilon)]^{1/3}}. \end{gathered} \tag{3.6}$$

The initial conditions for Eqs. (3.6) for $t_0 = 0$ will be $x_0 = 1$ and $y_0 = p_0\varepsilon/\rho_0 a_0^2$.

The asymptotic solution of (3.6) for $x \gg 1$ was obtained in [14]. In this case $a/R = \varepsilon^{1/3}$ and Eq. (3.6) can be easily integrated. Since we are studying the near zone ($x \sim 1$), such a solution is not applicable. The camouflet equation (3.6) can be solved numerically on a computer, but an approximate analytic solution is also possible. In order to solve the camouflet equation (3.6), the nonintegrable factors in it were replaced by interpolating integrable expressions. These expressions were chosen so that the asymptotic behavior of the exact solution of Eq. (3.6) and the interpolated solution coincided for $x \gg 1$ and for $x = 1$. The interpolated solution of the camouflet equation (3.6) constructed in this manner has the form

$$y(x) = \frac{2(1-\varepsilon)p_0}{\rho_0 a_0^2}\left(\frac{x-1+\varepsilon}{x-1}\right)^2\left\{x^{-3\gamma}\left[\frac{1}{\varepsilon x^{1/\varepsilon}}\left(\frac{x}{2\mu - 3\gamma - \frac{1}{\varepsilon} + 1} - \right.\right.\right.$$

$$-\frac{1}{2\mu-3\gamma-1/\varepsilon}\Big)+\frac{1}{1-\varepsilon^{1/3}}\Big(\frac{1}{2\mu-3\gamma}-\frac{1}{x^3(2\mu-3\gamma-3)}\Big)\Big]$$

$$+x^{-2\mu}\Big[\frac{1}{\varepsilon}\frac{1}{\Big(2\mu-3\gamma-\frac{1}{\varepsilon}+1\Big)\Big(2\mu-3\gamma-\frac{1}{\varepsilon}\Big)}+\frac{3}{(1-\varepsilon^{1/3})(2\mu-3\gamma)(2\mu-3\gamma-3)}\Big]\Big\}, \tag{3.7}$$

$$\mu=\frac{3/2-\varepsilon^{1/3}-\frac{1}{2}\varepsilon^{4/3}}{1-\varepsilon^{1/3}}.$$

Comparison of the solution (3.7) with the exact numerical solution of Eq. (3.6) shows that they agree satisfactorily (the deviation of the interpolation solution from the exact solution does not exceed 15% over the entire range of variation in x). For $x \gg 1$, the solution (3.7) transforms into the solution obtained in [14]. Using solution (3.7), we obtain the law governing the damping of the shock wave amplitude

$$p(R)=\frac{\rho_0 a_0^2}{\varepsilon}\Big(\frac{a}{R}\Big)^4 y(x)=\frac{\rho_0 a_0^2 \varepsilon^{1/3} x^4 y(x)}{[x^3-(1-\varepsilon)]^{4/3}} \tag{3.8}$$

and the energy dissipated on the shock front

$$E(x)=\frac{1}{2}p(x)\frac{\varepsilon}{\rho_0}=\frac{a_0^2\varepsilon^{4/3}x^4 y(x)}{2[x^3-(1-\varepsilon)]^{4/3}}. \tag{3.9}$$

In order to provide a physical interpretation of the computational results using the chosen models [14], it is assumed that the compaction ε is related to irreversible pore collapse. In this case, it is found that $\varepsilon = m$, where m is the initial porosity. The medium behind the shock wave in all the calculations was assumed to be nonporous with density $\rho_1 = 2.65$ g/cm^3; at the same time, E(x), defined by Eq. (3.9), will represent the internal thermal energy of the medium. According to [18], the specific internal thermal energy is the criterion for solid–liquid and liquid–vapor phase transitions. Some range of values of this energy corresponds to a mixed state of phases. Let E_B be the upper limit of the energy interval for the solid–liquid phase transition, i.e., E_B is the minimum specific energy for which the matter can exist in a completely melted state, and E_H is the lower limit for a liquid–gas phase transition. Specific values of these quantities were chosen as follows: $E_B = 500$ kJ/kg and $E_H = 4000$ kJ/kg.

Figure 9 shows the internal thermal energy of the medium as a function of the quantity r/a_0 for different porosities (curve 1 corresponds to m = 6%; 2, 20%; 3, 30%; 4, 50%; and 5, 60%), computed from Eq. (3.9). If the mutual positions of curves 1-3 are compared, then it is evident that initially, as the porosity increases, the amount of thermal energy increases monotonically. For a porosity m > 50%, the thermal energy near the cavity continues to increase, while for large values of the radius ($r/a_0 \sim 3$-4), due to the strong damping of the shock wave, the quantity of thermal energy becomes less than for porosities m < 50%. The dependences illustrated in Fig. 9 permit determining the mass of the melt and the fraction of the total energy in the explosion η contained in it as a function of porosity. These dependences are shown in Figs. 10 and 11, respectively (curve 1 in both figures). Curve 1 in Fig. 10 indicates the fact that the mass of the melt increases strongly with an increase in porosity over the range 0 < m < 20%. For 20% < m < 40%, the mass of the melt remains practically unchanged, while for m > 40% it begins to decrease. Such behavior can be explained by the competing action

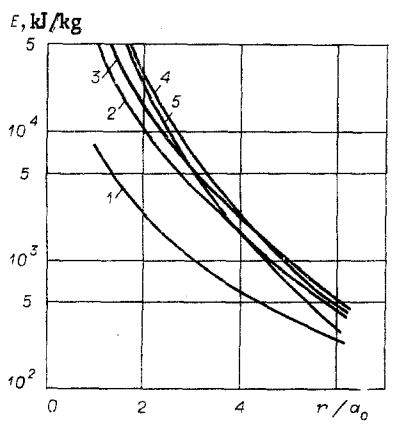

Fig. 9

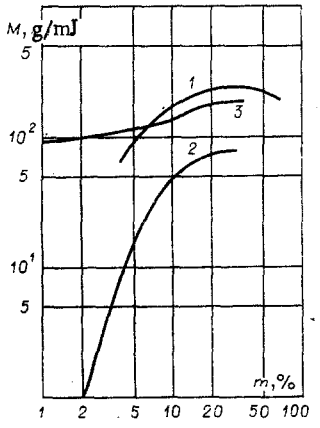

Fig. 10

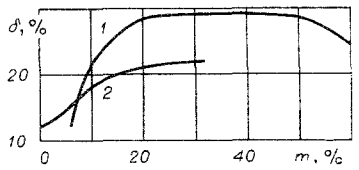

Fig. 11

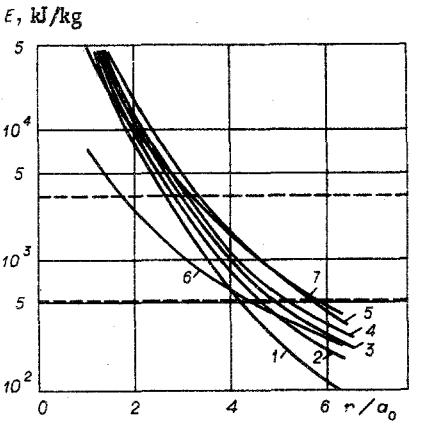

Fig. 12

of two mechanisms. The energy of shock compression is proportional to the product of the shock wave amplitude p(R) and the compaction on the shock front ε. As the porosity increases, ε increases, and p(R) decreases as a result of the increase in energy dissipation. For low porosities, the increase in ε prevails over the decrease in p(R), and for large values, vice versa. Curve 1 in Fig. 11 has the same form with a maximum. Calculations according to the model in [14] gives the maximum possible value for the heat energy of the melt as 30%. This value is attained for m ≈20% and remains unchanged up to m ≈50%.

The results of the calculations based on the model in [14] only give the correct qualitative understanding of the dissipative processes in the near zone of the explosion, since they do not take into account the variable compaction of the medium on the shock front and subsequent expansion of the medium behind the shock front, which is most important for low porosities. In order to take into account these factors, it is necessary to solve the system of equations (3.1)-(3.3) numerically on a computer. In the present work, this system of equations was solved numerically with the help of the difference scheme described in Sec. 1. The medium before the explosion was assumed to be porous and containing pores saturated with gas. With compression, the pore space on the shock front is sorted out and further compression occurs with the continuous material. The continuous material was described by a Mie–Gruneisen equation of state [18] with the following parameters: initial density 2.65 g/cm^3, plastic velocity of sound 4500 m/sec, and Gruneisen coefficient 1.

The numerically computed dependence of the thermal energy of shock compression on distance is presented in Fig. 12 (curve 1 corresponds to m = 0; 2, 6%; 3, 10%; 4, 20%; 5, 30%). Curves 6 and 7 represent curves 1 and 2 in Fig. 9 and are drawn for a comparison. The dashed lines separate out the melted zone. A zone with partially or completely vaporized rock, which can be assumed to be the gas cavity formed with the explosion, is located above the upper line. Expanding, this gas cavity gives up part of its energy to the surrounding medium in the form of kinetic energy and work on overcoming the strength forces. However, as numerical calculations show, considerable expansion of the vaporized rock will occur already after the shock wave passes the boundary of the entire melt zone. With further expansion of the gas cavity, the melt zone will not increase, since the melting is relayed to shock heating and the amplitude of the shock wave by this time will be less than that required for melting.

It is evident from Fig. 12 that in the range of porosities studied (0 < m < 30%) the amount of thermal energy increases with increasing m. Comparison of curves 2 and 6, as well as 4 and 7, indicates that calculations based on the model in [14] for low porosities underestimate energy dissipation, while for high porosities they overestimate it. This is already evident from the results presented in Fig. 11, where curve 2 indicates the fraction η of the thermal energy out of the total energy of the explosion in the melt. As the porosity increases, with m > 25%, this curve becomes asymptotic, equal approximately to 22%. Thus, the maximum possible heat energy transferred to the melt can be 22% of the overall energy of the explosion. Curve 2 in Fig. 10, illustrating the increase in mass of the melt in comparison with a nonporous medium (i.e., $M - M_0$, where M_0 is the mass of the melt with m = 0), also becomes a horizontal asymptote for high porosities. Analysis of the numerical results indicates the fact that for low porosities 0 < m < 8% the amount of melt increases according to a power law

$$M = 98 + 0.25m^{2.4}. \tag{3.10}$$

Curve 3 indicates the dependence of the total quantity of melt on the porosity, obtained with the help of numerical calculations. Comparison of curves 1 and 3 shows that the model in [14] underestimates the mass of the melt for low values of m and overestimates it for high porosities.

Let us briefly summarize the main results. Solution of the system of equations (3.1)-(3.3) with the help of the model in [14] and its numerical integration gives the mass of the melt and its thermal energy as a function of the porosity, which agree qualitatively. The characteristic feature of both dependences is the presence of an extremum for m ~20-40%. According to numerical calculations, the quantity of heat energy in the melt cannot exceed 22% of the total energy in the explosion. For low porosities, the mass of the melt increases according to a power law (3.10).

4. Explosion in a Medium with Radially Nonuniform Strength Properties. When explosions are set off in massive rocks, spatial nonuniformity of the strength properties of the rocks is often encountered. This nonuniformity can be related to the change in the physicomechanical properties of the rock (e.g., due to the difference in porosity or nature of saturation of the pore space: gas or liquid), as well as to the change in its chemical composition. Under natural conditions, such nonuniformity usually has a layered spatial structure, i.e., it consists of alternating strata of different rocks or a single stratum, but with different mechanical properties. However, the nonuniformity of physicomechanical properties can also have a radial character. For example, radial nonuniformity arises after an underground camouflet explosion. If two successive explosions are set off at the same location, then the stress wave arising with the second explosion will propagate through the cavity or the medium partially destroyed by the first explosion, which has a definite effect on the dynamics of the development of the second explosion. At this point, we will examine the effect of radial nonuniformity in the physicomechanical properties of the medium near a camouflet cavity, created by the first explosion, on the development process of the second explosion.

We will assume that the radial nonuniformity is created as a result of the first explosion in the medium saturated primarily by liquid and having some gaseous porosity. We assume that failure of the material in the medium occurs on the front of a plastic wave [14]. Some time after the first explosion, the pore liquid wets the contacts between the crushed pieces and decreases the coupling. For this reason, the coupling in the plastic flow zone due to the first explosion, which we will refer to as the failure zone of the medium, will be considerably less than in the medium with no failure. Moreover, it is well known [19] that the liquid-saturated medium shows almost no strengthening properties such as dry friction. For this reason, it may be assumed that in the failure zone arising with the first explosion the tangential stresses arising with the second explosion are absent. We will refer to this zone as the first zone (zone 1). We will denote its initial and instantaneous radii as b_0 and b, respectively. In the failure-free zone (zone 2), the tangential stresses arising with the second explosion differ from zero. We will assume that the cavity formed after the first explosion is filled by the pore liquid and pieces of crushed rock.

Now, a second explosion is set off in this preformed medium, which we will describe as follows. Assume that initially the energy of the second explosion W is liberated in a spherical region with dimension a_0. We will assume that the matter in the cavity is an ideal gas with a constant adiabatic index $\gamma=1.4$. In order to describe the motion of the medium, it is necessary to use a system of hydrodynamic equations (1.1) and (1.2) that takes into account the strength effects. The plastic properties of the medium were taken into account using Coulomb's law (2.1).

The system of equations indicated can be solved exactly only by numerical methods. However, in order to understand the effects accompanying the second explosion qualitatively, it can be solved within the framework of the model in [14]. Following [14], we assume that matter is compressed irreversibly from the density ρ_0 to a density ρ_1 on the shock-wave front. This compression is characterized by the parameter $\varepsilon=1-\rho_0/\rho_1$. The medium behind the shock front is assumed to be incompressible and plastic. For this reason, the energy equation in (1.1) and Eq. (2.1) can be omitted. The boundary conditions on the cavity of the second explosion $a(t)$ and on the shock front $R(t)$ have the form

$$u(R)=\dot{R}\varepsilon,\ u(a)=\dot{a},\ \sigma_r(R)=-\rho_0 u^2(R)/\varepsilon-p_\infty,\qquad \sigma_r(a)=-p_0(a_0/a)^{3\gamma}, \tag{4.1}$$

where p_∞ is the back pressure; p_0 is the initial pressure in the cavity; a_0 is the initial size of the gas cavity ($a_0 \sim W^{1/3}$). We note that the compaction ε, arising on the front of the plastic wave, is related to closing of gas-saturated pores. The liquid, contained in the pores, is assumed to be incompressible.

Taking into account the condition for incompressibility behind the shock front, it follows from the equation of continuity that in both zones

$$u=\dot{a}a^2/r^2. \tag{4.2}$$

Substituting this relation into the equation of motion in system (1.1), integrating with respect to r and using the boundary conditions (4.1) on the cavity, we obtain the distribution of stresses in zone 1:

$$a \leqslant r \leqslant b, \quad -\sigma_r(r) = -\sigma_\varphi(r) = p(r) = \rho_1((\ddot{a}a^2 + 2a^2\dot{a})/r - \dot{a}^2a^4/2r^4) + p_0(a_0/a)^{3\gamma} - \rho_1(\ddot{a}a + (3/2)\dot{a}^2). \tag{4.3}$$

Integrating the equation of motion in system (1.1) taking into account (2.1), (4.1), and (4.2) for $b \leq r$, we obtain a similar distribution of stress in zone 2:

$$\sigma_r(r) = \frac{\sigma^*}{k} + \rho_2\left\{\frac{\ddot{a}a^2 + 2\dot{a}^2a}{(\alpha-1)r} - \frac{2\dot{a}^2a^4}{(\alpha-4)r^4}\right\} - \left(\frac{R}{r}\right)^\alpha\left\{\frac{\sigma^*}{k} + \rho_{20}\frac{\dot{a}^2}{\varepsilon_2}\left(\frac{a}{R}\right)^4 + p_\infty + \rho_2\left[\frac{\ddot{a}a + 2\dot{a}^2}{\alpha-1}\frac{a}{R} - \frac{2\dot{a}^2}{\alpha-4}\left(\frac{a}{R}\right)^4\right]\right\}, \tag{4.4}$$

$$\alpha = \frac{6k}{3+2k}, \quad \tau = -\frac{3\sigma^*}{3+2k} + \frac{3k}{3+2k}\sigma_r.$$

Knowing the law governing the propagation of the shock wave $R(t)$ and the law governing the expansion of the cavity $a(t)$, with the help of (4.3) and (4.4), it is possible to calculate the stress in the zone $a \leq r \leq R$. The function $a(t)$ is obtained from a solution of the camouflet equation. For $R(t) \leq b_0$, the camouflet equation is obtained if the boundary condition on the shock front (4.1) is substituted into (4.3), while for $R(t) > b_0$, the condition for continuity of the quantity σ_r at $r = b$ is used. The final camouflet equation has the following form:

for $R(t) \leq b_0$

$$\frac{dy}{dx} = \frac{1}{x\left(1-\frac{a}{R}\right)}\left\{\frac{2p_0}{\rho_1 a_0^2}\frac{1}{x^{3\gamma}} - \frac{2p_\infty}{\rho_1 a_0^2} - 2y\left[\frac{3}{2} - 2\frac{a}{R} + \frac{2-\varepsilon_1}{2\varepsilon_1}\left(\frac{a}{R}\right)^4\right]\right\},$$
$$\frac{dt}{dx} = \frac{1}{\sqrt{y}}, \quad x = \frac{a}{a_0}, \quad y = \dot{x}^2, \quad \frac{a}{R} = \frac{\varepsilon_1^{1/3}x}{\left[x^3 - (1-\varepsilon_1)\right]^{1/3}} \tag{4.5}$$

(the initial conditions for Eq. (4.5) at $t_0 = 0$ will be $x_0 = 1$ and $y_0 = p_0\varepsilon_1/\rho_0 a_0^2$);

for $R(t) \geq b$

$$\frac{dy}{dx} = \left\{x\left[\rho_1\left(1-\frac{a}{b}\right) + \rho_2\left(\frac{R}{b}\right)^\alpha\frac{1}{\alpha-1}\frac{a}{R} - \frac{\rho_2}{\alpha-1}\frac{a}{b}\right]\right\}^{-1}\left\{\frac{2p_0}{a_0^2}\frac{1}{x^{3\gamma}} - 2\frac{p_\infty}{a_0^2}\left(\frac{R}{b}\right)^\alpha - \frac{2}{a_0^2}\frac{\sigma^*}{k}\left[\left(\frac{R}{b}\right)^\alpha - 1\right] - 2y\left[\rho_1\left(\frac{3}{2} - 2\frac{a}{b} + \frac{1}{2}\left(\frac{a}{b}\right)^4\right)\right.\right.$$
$$\left.\left. - \rho_2\left(\frac{2}{\alpha-1}\frac{a}{b} - \frac{2}{\alpha-4}\left(\frac{a}{b}\right)^4\right) + \left(\frac{R}{b}\right)^\alpha\frac{\rho_{20}}{\varepsilon_2}\left(\frac{a}{R}\right)^4 + \left(\frac{R}{b}\right)^\alpha\rho_2\left(\frac{2}{\alpha-1}\frac{a}{R} - \frac{2}{\alpha-4}\left(\frac{a}{R}\right)^4\right)\right]\right\}, \tag{4.6}$$
$$\frac{dt}{dx} = \frac{1}{\sqrt{y}}, \quad \frac{a}{b} = \frac{x}{\left\{(1-\varepsilon_1)\left[\left(\frac{b_0}{a_0}\right)^3 - 1\right] + x^3\right\}^{1/3}},$$
$$\frac{a}{R} = \frac{\varepsilon_2^{1/3}x}{\left[x^3 - (\varepsilon_1-\varepsilon_2)\left(\frac{b_0}{a_0}\right)^3 - (1-\varepsilon_1)\right]^{1/3}}, \quad \frac{b}{R} = \left(\frac{a}{R}\right)\left(\frac{b}{a}\right).$$

The initial conditions for Eq. (4.6) at $t = t_1$ will be $y = y_1$ and $x = x_1 = \left[\varepsilon_1\left(\frac{b_0}{a_0}\right)^3 + (1-\varepsilon_1)\right]^{1/3}$, where t_1 is the time at which the shock wave arrives at the boundary of zone 2 ($R = b_0$), while y_1 is the value of y at this time obtained from the solution of (4.5). In Eqs. (4.5) and (4.6), ε_1, ρ_{10}, ρ_1, ε_2, ρ_{20}, and ρ_2 are the compaction and density in front of the shock wave and behind the shock wave in zones 1 and 2, respectively, which generally speaking can be different. Eqs. (4.5) and (4.6) were solved numerically on a computer with the following initial parameters: $p_0 = 800$ kbar, $\sigma^* = 500$ bar, $k = 0$, and $p_\infty = 200$ bar. The densities behind the shock front in zones 1 and 2 were assumed to be identical: $\rho_1 = \rho_2 = 2.7$ g/cm^3.

The results of the calculations are presented in Table 2, where R_1 is the radius of the failure zone. Within the framework of the model chosen [14], the position of the failure front is identified with the position of the shock front. For this reason, the position of the shock front at the time the cavity stops growing gives the maximum boundary for the failure zone. As is evident from Table 2, the compaction parameters in zones 1 and 2 and the relative radius of the zone with decreased strength b_0/a_0 were varied during the calculations. The variation in the parameter b_0/a_0 can be related to the different scales of the first and second explosions, since b_0 gives the size of the zone with zero strength properties, which is created by the action of the first explosion. The variant $b_0/a_0 = 0$ can be represented as a single explosion detonated in a radially uniform me-

TABLE 2

No. of series	ε_1	ε_2	$\frac{b_0}{a_0}$	$\frac{a_{max}}{a_0}$	$\frac{R_1}{a_0}$
1	0,01	0,02	20	12,3	45,0
			10	10,5	37,5
			5	9,65	35,0
			—	9,1	33,6
2	0,02	0,02	20	12,0	44,3
			10	10,2	37,5
			5	9,4	34,5
			—	9,1	33,6
3	0,01	0,04	20	13,2	40,0
			10	11,0	32,5
			5	10,0	29,3
			—	9,25	27,0

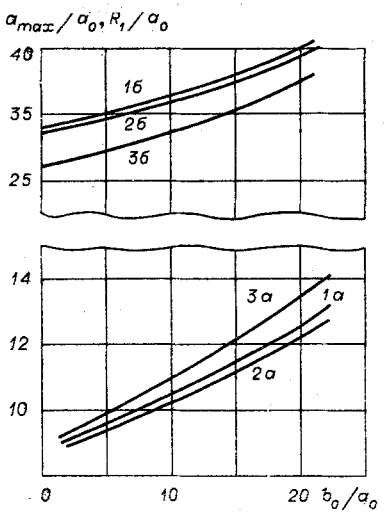

Fig. 13

dium with the parameters of zone 2. It is evident that as b_0/a_0 increases (i.e., as the scale of the first explosion relative to the second increases) in all the calculations the maximum cavity radius and the radius of the failure zone increases monotonically. Figure 13 shows the maximum cavity size a_{max}/a_0 and the boundary of the failure zone R_1/a_0 as a function of the quantity b_0/a_0. The number of the curve in Fig. 13 corresponds to the number of the series in Table 2. Curves 1a, 2a, and 3a correspond to the cavity radius, while curves 1b, 2b, and 3b correspond to the boundary of the failure zone. From Fig. 13, it is evident that the greatest increase in the dimensions of the cavity (curve 3a) occurs when the compaction in zone 2 is greater than in zone 1 (series, 3, Table 2). Analysis of the results presented in Fig. 13 leads to the conclusion that with the second explosion the maximum size of the cavity will be 1.3-1.5 times, and its volume 2.2-2.3 times, greater than for the first explosion with the same intensity. We note that this simplifled setup does not take into account the return motion of the cavity. Comparison of curves 1b-3b shows that the largest failure zone dimensions due to the second explosion occur for a medium with low initial gas porosity. This is related to the lower energy dissipation on the shock front due to the small value of the porosity. As b_0/a_0 increases, the value of R_1/a_0 increases monotonically. In comparison with the first explosion ($b_0/a_0 = 0$), this increase can attain 30-50%.

The solution of the problem of the explosion within the framework of the model proposed in [14] only gives the correct qualitative understanding of the basic effects accompanying the second explosion: Increase in the maximum radius of the cavity and increase in the failure zone. A more complete description of the

TABLE 3

No. of series	$\frac{W}{W_0}$	$\frac{d}{a_0}$	$\frac{b_0}{a_0}$	$\frac{a_{max}}{a_0}$	$\frac{R_1}{a_0}$	E_1	E_2	E_3	E_4	E_5	E_6	E_7	E_8
1	1	—	—	6,0	26,3	4,2 5,0	25 30	43 51	68 81	4,9 5,8	7,2 8,6	12,1 14,4	16
2	10	—	—	6,0	27,8	4,8 5,7	25 30	42 50	67 80	5,3 6,3	7,1 8,4	12,4 14,7	16
3	1	6,0	26	7,7	34	3,3 3,9	2,4 2,9	57 67	59 70	8,1 9,6	13,5 16,0	21,6 25,6	16
4	10	2,7	13,5	7,1	32,4	5,1 6,2	13 16	44 54	57 70	8,5 10,5	11 13,5	19,5 24	18
5	10	6,0	27,2	7,8	35,1	3,3 3,9	1,4 1,7	58 68	59 70	8.0 9,5	13 15,5	21 25	16

explosion in the medium with radially nonuniform strength properties can only be obtained with a numerical solution of the starting system of equations with the equation of state of the medium [6] reflecting the irreversible nature of the volume deformation [3-6], which was used in Secs. 1 and 2.

For the equation of state for a saturated porous medium [6], it is necessary to give a number of parameters characterizing the material of the matrix and the saturating liquid. The microscopic parameters were chosen as follows: density of the matrix 2.65 g/cm^3, plastic velocity of sound in the matrix 4500 m/sec, shear modulus $G_m = 100$ kbar, shear strength $Y = 1$ kbar. The following parameters were chosen for the pore liquid: density 0.85 g/cm^3, velocity of sound 1000 m/sec. In order to describe the macroscopic elastoplastic behavior of the porous medium as a whole the values of the constants entering into (1.2) and (2.1) were taken as follows: $G = 50$ kbar, $\sigma^* = 0.5$ kbar, $k = 0$. The back pressure was set equal to 500 bar in all calculations.

The results of the numerical computations are presented in Table 3. Here, calculations 1 and 2 represent the results of the first explosions in a radially uniform medium with energies W_0 and $10W_0$, respectively. Calculations 3 and 4 give the results for detonation of a second explosion with energy W_0 and $10W_0$, respectively, if the energy of the first explosion was W_0. Calculation 5 gives the results of the secondary explosion with energy $10W_0$, if the energy of the first explosion was also $10W_0$.

For the second explosion, the medium initially has the following complicated radial structure. For $0 \leq r \leq d$, there is a cavity created by the first explosion (d is the size of the cavity from the first explosion; in Table 3 for calculations 3 and 4 this is a_{max} for calculation 1 and for the variants 5, it is a_{max} from calculation 2). It is assumed that the medium filling this cavity consists of pieces of crushed rock that have fallen into the cavity and is porous with a bulk porosity of 75%. The pores are completely saturated with liquid. Furthermore, for $d \leq r \leq b_0$, there is a zone with low-strength properties (zone 1). In this zone, as in the simplified analysis, it is assumed that $\sigma^* = 0$ and $k = 0$. For $r > b_0$, it is assumed that the medium has strength properties ($\sigma^* = 0.5$ kbar and $k = 0$). The porosity of the medium in zones 1 and 2 is 11%. It is evident from Table 3 that for the second explosion there is a significant, compared to the first explosion, increase in the dimensions of the failure zone, which, as above, we will relate to the maximum radius of the plasticity zone. This increase is related to the large maximum dimensions of the cavity with repeated explosions and, as a result, to the large shear stresses in regions far removed from the center of the explosion. This also follows from Fig. 14, which shows the development of the cavity as a function of time (the curves are numbered in a manner corresponding to the enumeration of the calculations in Table 3). Comparison of curves 4 and 5 indicates that the maximum cavity radius and, therefore, the size of the failure zone depends only slightly on the scale of the first explosion, i.e., on the parameter b_0/a_0. The oscillatory growth of curves 4 and 5 in Fig. 14 indicates the presence of reflected rarefaction waves, arising with the passage of the main shock wave through the boundary of the cavity formed by the first explosion. This then leads, as shown by numerical calculations, to the appearance of secondary shock waves, propagating behind the primary wave. At the same time, cyclical stresses arise in the medium surrounding the old cavity, which can lead to an even greater damage to the medium. It should also be noted that the final dimensions of the cavity resulting from the repeated and initial explosions are nearly equal due to the strong return motion with the repeated explosion. The largest maximum radius and strong return motion of the cavity with the second explosion lead to total shear deformations that are 50% greater than for the first explosion with the same energy. This fact is important in studying processes related to shear deformation of a medium with an explosion.

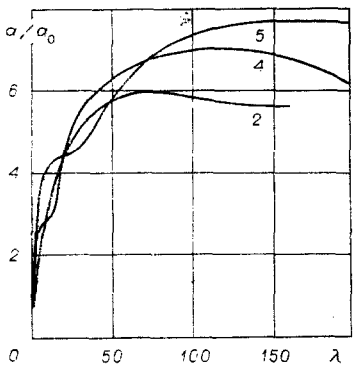

Fig. 14

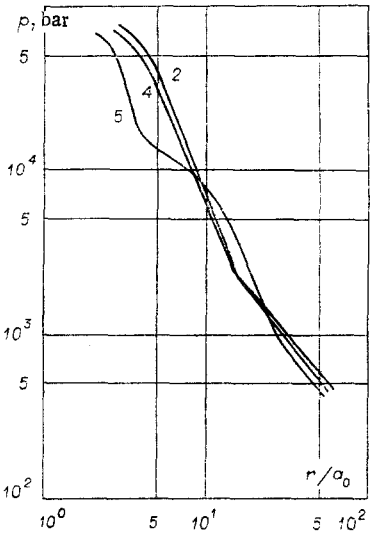

Fig. 15

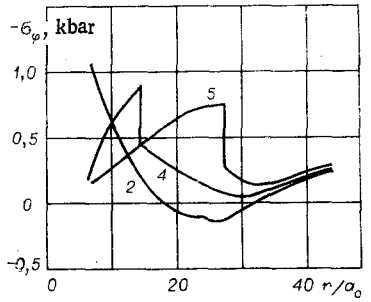

Fig. 16

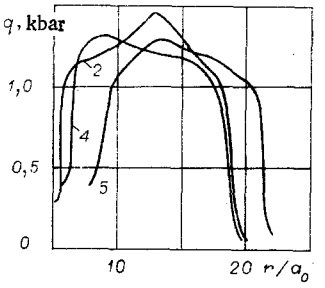

Fig. 17

The dependence of the peak pressure on distance for variants 2, 4, and 5 (enumeration as in Table 3) is shown in Fig. 15. The characteristic deviation in curve 5 is related to the passage of the shock wave through the boundary of the cavity formed by the first explosion. The absence of a clearly visible deviation in curve 4 is related to the small dimensions of the cavity formed by the first explosion for this variant of the calculation. In zone 1, the amplitude of the shock wave with the second explosion is greater, and in zone 2 smaller, than from the first explosion with the same intensity. Figure 16 shows the dependence of the azimuthal stress σ_φ on the distance at a time when the gas cavity formed by the explosion stops expanding; it is evident that one feature of the first explosion for the chosen parameters of the medium and back pressure is the presence of a zone, behind the plasticity zone, with azimuthal tensile stresses, which can be identified with a radial fracture zone [20, 21]. The results of the calculations show that with repeated explosions such a zone is not formed due to the presence of a region with low strength. Thus, it is difficult to obtain a radial fracture region with a repeated explosion. The jump in curves 4 and 5 is related to the boundary between zones 1 and 2. Analysis of curves 2, 4, and 5 shows that the azimuthal stresses with repeated explosions are greater than for the first explosions.

The equation of state of the medium used in the present work [6] permits obtaining the distribution of the pore pressure after an explosion. Figure 17 shows these dependences for explosions 2, 4, and 5, and it is evident that as a result of the explosion a zone with high pore pressure is formed. According to [4-6], its appearance is related to partial pore filling at the compression phase with the passage of the shock wave. The presence of a zone with increased pore pressure can have an important effect on the filtration properties after the explosion. It is evident from Fig. 17 that the size of this zone is somewhat greater for the second explosion than for the first explosion.

Table 3 also shows the characteristics of the dissipative processes for the initial and repeated explosions. All energy values correspond to a time when the cavity has stopped expanding. The energies are labeled as in Table 1. It is evident from Table 3 that the fraction of the energy dissipated on the shock front, as well as the kinetic energy of the medium and energy of the gases in the cavity for the first and repeated explosions, are nearly equal. The value of E_2 and, as a result, that of E_4 are significantly less for the re-

peated explosions. This is related to the presence of zone 1, where there are no tangential stresses and where the shear is much greater than in zone 2. As a result, the stored elastic energy E_5 is much higher. The energy stored in this manner returns to the medium in the form of kinetic energy and energy of compression of gases in the cavity during the return motion of the cavity. This is one of the reasons for the strong return motion of the cavity with the repeated explosion. Thus, the repeated explosion is characterized, compared to the first explosion, by a smaller fraction of energy dissipated into heat and a greater residual elastic energy. Analysis of the dynamic effects of the repeated explosion in a porous saturated medium leads to the following results: increased maximum radius of the cavity and failure zone; larger dimensions of the zone with high pore pressure; appearance of cyclical stresses in the vicinity of the cavity formed by the first explosion and even greater destruction of the medium; shear stresses with repeated explosions, presented in Table 3, 50% greater than stresses arising with an initial explosion with the same energy. The calculations showed that for the repeated explosion there is a strong return motion of the cavity.

In conclusion, the authors thank V. N. Nikolaevskii for the suggestion of examining the dissipation of energy in the near zone of an explosion and V. I. Musinov for suggesting an analysis of the effects of the repeated explosion in a porous medium. The authors are grateful to S. Z. Dunin and V. V. Surkov for presenting them with the results of [6] before publication. The authors are grateful to V. K. Sirotkin for many useful remarks and discussion of the work.

LITERATURE CITED

1. T. R. Butkovich, "Influence of water in rocks on the effects of underground nuclear explosions," in: Underwater and Underground Explosions [Russian translation], Mir, Moscow (1974).
2. E. E. Lovetskii, A. M. Maslennikov, and V. S. Fetisov, "Expansion of a gas cavity in gas- and water-saturated elastoplastic medium," Prikl. Mekh. Tekh. Fiz., No. 1 (1979).
3. S. S. Grigoryan, "Basic ideas concerning the dynamics of soils," Prikl. Mat. Mekh., 24, No. 6 (1960).
4. M. M. Carroll and A. S. Holt, "Static and dynamic pore collapse relation for ductile porous materials," J. Appl. Phys., 43, No. 4 (1972).
5. J. J. Bhatt, M. M. Carroll, and J. F. Shatz, "A spherical model calculation for volumetric response of porous rocks," J. Appl. Mech., 42, No. 2 (1975).
6. S. Z. Dunin and V. V. Surkov, "Equations of state of a gas- and water-saturated medium," Izv. Akad. Nauk SSSR, Ser. Fiz. Zemli, No. 11 (1978).
7. V. N. Nikolaevskii, K. S. Basniev, A. T. Gorbunov, and G. A. Zotov, Mechanics of Saturated Porous Media [in Russian], Nedra, Moscow (1970).
8. Physics of Explosions [in Russian], Nauka, Moscow (1975).
9. V. M. Kuznetsov, "Average size of pieces formed in crushing rocks with an explosion," Fiz.-Tekh. Probl. Razrab. Polezn. Iskop., No. 2 (1973).
10. B. D. Khristoforov, L. D. Lifshits, I. V. Belinskii, and A. N. Averin, "Influence of porosity on the parameters of dynamic compression of NaCl," Izv. Akad. Nauk SSSR, Ser. Fiz. Zemli, No. 8 (1971).
11. M. L. Wilkins, "Calculation of elastoplastic flows," in: Computational Methods in Hydrodynamics [Russian translation], Mir, Moscow (1967).
12. E. E. Lovetskii, A. M. Maslennikov, and V. S. Fetisov, "Spherical explosion in radially nonuniform saturated porous medium," Fiz. Goren Vzyrva, No. 3 (1979).
13. I. V. Belinskii and B. D. Khristoforov, "Energy dissipation in an underground explosion," in: Explosion Work, No. 76/33 (1976).
14. A. S. Kompaneets, "Shock waves in plastically compacting medium," Dokl. Akad. Nauk SSSR, 109, No. 1 (1956).
15. É. A. Koshelev, "Dissipation of energy in an underground explosion," Prikl. Mekh. Tekh. Fiz., No. 5 (1972).
16. S. S. Grigoryan, "Solution of the problem of an underground explosion in soft soils," Prikl. Mat. Mekh., 28, No. 6 (1964).
17. E. E. Lovetskii, A. M. Maslennikov, and V. S. Fetisov, "Energy dissipation with an explosion in a porous elastoplastic medium," Prikl. Mekh. Tekh. Fiz., No. 6 (1979).
18. Ya. B. Zel'dovich and Yu. P. Raizer, Physics of Shock Waves and High-Temperature Hydrodynamic Phenomena [in Russian], Nauka, Moscow (1966).
19. V. N. Nikolaevskii, "Mechanical properties of soils and the theory of plasticity," Ser. Mekh. Tverd. Deform. Tela, 6, VINITI Akad. Nauk SSSR (1972).
20. V. P. Koryakov, "Some ideas concerning the fracture zone and front," Dokl. Akad. Nauk SSSR, 114, No. 6 (1962).

21. A. B. Bagdasyaryan, "Exact solutions of problems concerning the action of an explosion in a brittle hard medium," Izv. Akad. Nauk ArmSSR, Ser. Mekh., 21, Nos. 5, 6 (1968).

EXPLOSION IN A GRANULAR POROUS MEDIUM WITH VARIABLE DILATANCY

E. E. Lovetskii, V. K. Sirotkin, and E. V. Sumin

UDC 622.235.5+539.374

Correct description of the flow of a granular medium is very important in considering an explosion in a granular or brittle rock. The most important feature of the flow of such a medium arises from repacking effects, which result not only in shear deformation but also in irreversible bulk strain. Usually, this bulk deformation is described within the framework of a dilatancy model [1]. The magnitude and sign of the dilatancy velocity are substantially dependent on the pressure and density [2-5]. It is assumed at present [6-9] that the dilatancy velocity is constant for such a medium. However, such an assumption does not allow one to incorporate the real dynamic behavior of the medium or to consider the effects of the initial state on the results of the explosion.

Here we process experimental data to derive an expression for the dilatancy velocity as a function of the pressure and density. This result is used in determining the expansion of a spherical gas cavity in an elastoplastic dilating medium. Particular attention is given to the final characteristics of the medium near the cavity. No allowance is made for the strength difference between the undisrupted and disrupted media, although this can be done if one assumes that the adhesion is small by comparison with the dry friction.

1. We consider spherically symmetrical motion in an elastoplastic porous dilating medium, which is compressed by a lithostatic pressure p_h. The source of the motion is a cavity of initial radius a_0 filled with adiabatically expanding explosion gases of initial pressure p_0 and adiabatic parameter γ.

The motion is described by the equation of continuity and the equation of motion:

$$\frac{\partial \rho}{\partial t} + u\frac{\partial \rho}{\partial r} + \rho\left(\frac{\partial u}{\partial r} + 2\frac{u}{r}\right) = 0; \tag{1.1}$$

$$\rho\left(\frac{\partial u}{\partial t} + u\frac{\partial u}{\partial r}\right) = -\frac{\partial p}{\partial r} + \frac{4}{3}\frac{\partial \tau}{\partial r} + \frac{4\tau}{r}, \tag{1.2}$$

where r is the distance from the explosion center, t is the time, u is the mass velocity, and ρ is the current density. The tangential stress τ and the pressure p are given by $\tau = (1/2)(\sigma_r - \sigma_\varphi)$, $p = -(1/3)(\sigma_r + 2\sigma_\varphi)$, where σ_r and σ_φ are the radial and azimuthal components of the stress tensor.

The stress variation in the elastic-strain zone is related to the velocity by Hooke's law:

$$\frac{d\tau}{dt} = G\left(\frac{\partial u}{\partial r} - \frac{u}{r}\right), \quad \frac{dp}{dt} = -K\left(\frac{\partial u}{\partial r} + 2\frac{u}{r}\right), \tag{1.3}$$

where $d/dt = \partial/\partial t + u\partial/\partial r$, G is the shear modulus, and K is the bulk compression coefficient.

Plastic strain will occur if the condition for plastic flow is met. We take this condition in the Mises–Huber–Schleicher form:

$$\frac{2}{\sqrt{3}}|\tau| = \alpha(\Lambda)p + Y, \tag{1.4}$$

where $\alpha(\Lambda)$ is the coefficient of friction, which is dependent on the dilatancy velocity Λ and Y is the adhesion. The $\alpha(\Lambda)$ dependence has been derived in [1] by processing data for various types of sands and takes the form

$$\alpha(\Lambda) = \frac{1}{2.11}(1.52 + 1.38\Lambda - \Lambda^2). \tag{1.5}$$

Moscow. Translated from Zhurnal Prikladnoi Mekhaniki i Tekhnicheskoi Fiziki, No. 2, pp. 149-155, March-April, 1981. Original article submitted January 10, 1980.

0021-8944/81/2202-0266$07.50